Patterns of reproductive isolation in a haplodiploid – strong postmating, prezygotic barriers among three forms of a social spider mite

Sato, Y.; Sakamoto, H.; Gotoh, T.; Saito, Y.; Chao, J.-T.; Egas, M.; Mochizuki, A.

DOI
10.1111/jeb.13270

Publication date
2018

Document Version
Final published version

Published in
Journal of Evolutionary Biology

JOURNAL OF Evolutionary Biology

doi: 10.1111/jeb.13270

Patterns of reproductive isolation in a haplodiploid – strong post-mating, prezygotic barriers among three forms of a social spider mite

YUKIE SATO*† , HIRONORI SAKAMOTO‡§, TETSUO GOTOH‡, YUTAKA SAITO¶, JUNG-TAI CHAO**, MARTIJN EGAS†† & ATSUSHI MOCHIZUKI†

*Sugadaira Research Station, Mountain Science Center, University of Tsukuba, Ueda, Nagano, Japan
†Institute for Agro-Environmental Sciences, NARO, Tsukuba, Ibaraki, Japan
‡Laboratory of Applied Entomology and Zoology, Faculty of Agriculture, Ibaraki University, Ami, Ibaraki, Japan
§Organization for University Research Initiatives, Waseda University, Shinjuku-ku, Tokyo, Japan
¶Research Faculty of Agriculture, Hokkaido University, Kita-ku, Sapporo, Hokkaido, Japan
**Division of Forest Protection, Taiwan Forestry Research Institute, Taipei, Taiwan
††Institute for Biodiversity and Ecosystem Dynamics, University of Amsterdam, Amsterdam, The Netherlands

Keywords:

cryptic reproductive isolation;
genetic distance;
haplodiploidy;
speciation.

Abstract

In speciation research, much attention is paid to the evolution of reproductive barriers, preventing diverging groups from hybridizing back into one gene pool. The prevalent view is that reproductive barriers evolve gradually as a by-product of genetic changes accumulated by natural selection and genetic drift in groups that are segregated spatially and/or temporally. Reproductive barriers, however, can also be reinforced by natural selection against maladaptive hybridization. These mutually compatible theories are both empirically supported by studies, analysing relationships between intensity of reproductive isolation and genetic distance in sympatric taxa and allopatric taxa. Here, we present the – to our knowledge – first comparative study in a haplodiploid organism, the social spider mite *Stigmaeopsis miscanthi*, by measuring premating and post-mating, pre- and post-zygotic components of reproductive isolation, using three recently diverged forms of the mite that partly overlap in home range. We carried out cross-experiments and measured genetic distances (mitochondrial DNA and nuclear DNA) among parapatric and allopatric populations of the three forms. Our results show that the three forms are reproductively isolated, despite the absence of premating barriers, and that the post-mating, prezygotic component contributes most to reproductive isolation. As expected, the strength of post-mating reproductive barriers positively correlated with genetic distance. We did not find a clear pattern of prezygotic barriers evolving faster in parapatry than in allopatry, although one form did show a trend in line with the ecological and behavioural relationships between the forms. Our study advocates the versatility of haplodiploid animals for investigating the evolution of reproductive barriers.

Introduction

The evolution of reproductive barriers, promoting diverging groups to form separate gene pools, has received much attention as a speciation mechanism which bridges microevolution and macroevolution (Futuyma, 1998; Howard & Berlocher, 1998; Coyne & Orr, 2004). Reproductive barriers may evolve in various modes; however, the most prevalent view is that it evolves gradually as a by-product of genetic changes accumulated by natural selection and genetic drift, whereas groups are segregated spatially or temporally (Futuyma, 1998; Howard & Berlocher, 1998; Coyne &

Correspondence: Yukie Sato, Sugadaira Research Station, Mountain Science Center, University of Tsukuba, Ueda, Nagano 386-2204, Japan.
Tel.: +81 (0)268 74 2002; fax: +81 (0)268 74 2016;
e-mail: uchietan@gmail.com

Orr, 2004). This view is supported by comparative analyses showing a positive relationship between intensity of reproductive isolation and genetic distance among groups (Coyne & Orr, 1989, 1997; Sasa *et al.*, 1998; Presgraves, 2002; Price & Bouvier, 2002; Moyle *et al.*, 2004; Scopece *et al.*, 2007; Malone & Fontenot, 2008; Yukilevich, 2012; Sánchez-Guillén *et al.*, 2014; Turelli *et al.*, 2014). Yet, the comparative analyses also support other view that prezygotic reproductive barriers are the result of natural selection to prevent maladaptive hybridization, by showing faster evolution of prezygotic isolation in sympatric taxa compared to allopatric taxa (Coyne & Orr, 1989, 1997). This is typically inferred from the slopes of regression lines of reproductive isolation intensity on genetic distance, assuming genetic distance is a proxy for divergence time. To help disentangle whether both mechanisms are involved in speciation, it is worthwhile to characterize the relationship between reproductive isolation and genetic distance for the various types of reproductive barriers between taxa.

Here, we address the evolution of reproductive barriers in a social spider mite, *Stigmaeopsis miscanthi* (Saito) (Acari: Tetranychidae). The social spider mite is a tiny arthropod herbivore (body size < 1 mm) infesting Chinese silver grass, *Miscanthus sinensis* Andersson. This mite species forms colonies by constructing woven nests from silk webbing on the undersurface of host plant leaves, and adult males, females and their offspring live in groups on the leaf surface covered by the silk webbing. When their natural enemies (mainly, predatory mites) intrude the nests, adult males and females counterattack and sometimes kill the natural enemies to protect their offspring and nest mates (Yano *et al.*, 2011). Males are aggressive not only to their natural enemies but also to conspecific males inside the nests, and even kill rival males to establish their own harem (Saitō, 1990). The frequency of male-killing (hereafter, male–male aggression) varies among populations (Saito, 1995; Sato *et al.*, 2013a), and recent researches have been revealing that the populations can be classified into at least three forms that differ in male–male aggression and weapon size (Saito & Sahara, 1999; Y. Sato, Y. Tsuda, H. Sakamoto, M. Egas, T. Gotoh, Y. Saito, Y-X. Zhang, J-Z. Lin, J-T. Chao & A. Mochizuki, unpublished). They differ in DNA sequences [18S and 28S rDNA, COI mitochondrial DNA (mtDNA) and the para-sodium channel genes] (Ito & Fukuda, 2009; Sakagami *et al.*, 2009; Sakamoto *et al.*, 2017; Y. Sato, Y. Tsuda, H. Sakamoto, M. Egas, T. Gotoh, Y. Saito, Y-X. Zhang, J-Z. Lin, J-T. Chao & A. Mochizuki, unpublished); therefore, their descriptions as different species are currently in progress (Saito *et al.*, 2018). Two distinct forms, the high aggression (HG) form and the low aggression (LW) form, are distributed in warmer and cooler Japanese regions, respectively (Saito & Sahara, 1999; Sato *et al.*, 2013a). In south-eastern Japan (Shizuoka Prefecture to Kagoshima Prefecture), they are parapatrically distributed with the HG form in the lowlands and the LW form in the highlands. At intermediate altitudes, their distributional ranges overlap and they were found in the same grass stands (Sato *et al.*, 2008). Another form, the so-called mild aggression (ML) form, was found recently in subtropical areas in Japan (the Southern Ryukyus), Taiwan and Fujian Province in China (Y. Sato, Y. Tsuda, H. Sakamoto, M. Egas, T. Gotoh, Y. Saito, Y-X. Zhang, J-Z. Lin, J-T. Chao & A. Mochizuki, unpublished). Its male weapon size is intermediate between the values for those traits in the HG and LW forms; therefore, it is not easy to discriminate it from the other two forms (Saito *et al.*, 2018; Y. Sato, Y. Tsuda, H. Sakamoto, M. Egas, T. Gotoh, Y. Saito, Y-X. Zhang, J-Z. Lin, J-T. Chao & A. Mochizuki, unpublished). However, naturally occurring populations of this form are geographically isolated from populations of other forms (Saito & Sahara, 1999; Y. Sato, Y. Tsuda, H. Sakamoto, M. Egas, T. Gotoh, Y. Saito, Y-X. Zhang, J-Z. Lin, J-T. Chao & A. Mochizuki, unpublished), and its DNA sequences (18S and 28S rDNA, COI mtDNA and para-sodium channel genes) are different from the other two forms (Sakamoto *et al.*, 2017; Y. Sato, Y. Tsuda, H. Sakamoto, M. Egas, T. Gotoh, Y. Saito, Y-X. Zhang, J-Z. Lin, J-T. Chao & A. Mochizuki, unpublished).

Spider mites are haplodiploid: the females develop from fertilized eggs and males develop from unfertilized eggs, and unmated females produce eggs that develop into sons (arrhenotokous parthenogenesis). In *S. miscanthi*, oviposition of virgins is significantly lower than that of fertilized females (Sato *et al.*, 2000a, b). Therefore, this mite species lends itself very well to study the various types of reproductive isolation: they can be directly assessed from oviposition rate, sex ratio in the offspring and offspring mortality. Low oviposition rate by cross-mated females (similar to virgin oviposition) indicates a premating reproductive barrier, overproduction of sons indicates a post-mating, prezygotic barrier and increased offspring mortality indicates a post-zygotic barrier (which can only affect survival of daughters as sons arise from unfertilized eggs). In spider mites, post-mating, prezygotic barriers (overproduction of haploid sons) are often found between conspecific strains and between closely related species including the HG and LW forms of *S. miscanthi* in parapatry (e.g. Takafuji & Fujimoto, 1985; Gotoh, 1986; Gotoh & Noguchi, 1990; Gotoh & Takayama, 1992; Gotoh *et al.*, 1995, 2005; Navajas *et al.*, 2000; Sato *et al.*, 2000a, b, 2014; Perrot-Minnot *et al.*, 2004). Much less is known, however, of the occurrence of premating reproductive barriers (e.g. Sato *et al.*, 2015; Clemente *et al.*, 2016) or post-zygotic barriers (e.g. Osakabe & Komazaki, 1996; Gotoh *et al.*, 2009; Knegt *et al.*, 2017), even though the detection of genetic incompatibilities is facilitated in haplodiploid organisms compared to diploids (Knegt *et al.*, 2017). Hence, documenting the different types of

reproductive barriers among the three forms of *S. miscanthi* not only allows comparative study of the speciation process but also allows the subsequent search for incompatibility genes. Both aspects are strongly underrepresented in the literature on speciation (Coyne & Orr, 2004; Maheshwari & Barbash, 2011; Nosil & Schluter, 2011; The Marie Curie Speciation Network, 2012).

In this study, we tested whether genetic distance explains the strength of reproductive isolation and whether geographic distribution affects evolution of reproductive isolation in *S. miscanthi* using four populations of each of the HG, LW and ML forms from the Korean Peninsula to the Taiwan Islands via the Kyushu and the Ryukyu Islands. Moreover, as the bacterial endosymbiotic reproductive manipulators *Wolbachia*, *Cardinium*, *Spiroplasma* have been previously reported in several spider mite species (Gotoh *et al.*, 2005, 2007; Ros & Breeuwer, 2009; Zhu *et al.*, 2012; Zhang *et al.*, 2016; Staudacher *et al.*, 2017), we also checked for their presence in the populations.

Materials and methods

Mites and host plants

In March 2009, we collected a whole plant of Chinese silver grass, *M. sinensis* Andersson, in Tsukuba (Ibaraki Prefecture, Japan). Its roots were pulled apart, and the resulting clones were grown in a greenhouse to be used for mite rearing and experiments. Populations of the social spider mite, *S. miscanthi* (Saito), were collected from the Korean Peninsula to the Taiwan Islands via the Kyushu Islands and the Ryukyu Islands (Fig. 1). We divided the area into five according to the presence of the various forms of the spider mite, current faunal characteristics and geographic features: LW area (the Korea Peninsula), HG + LW area (where HG and LW populations parapatrically occur in the Kyushu region), HG area (the Central Ryukyus), ML area in Japan (the Southern Ryukyus) and ML area in Taiwan (the Taiwan Islands). Populations were collected from two sites in LW area, HG area, Japanese ML area and Taiwan ML area, and two HG populations and two LW populations were collected in the HG + LW area (Fig. 1). In total, 12 populations were obtained by mite collection from December 2008 to July 2009. Collected mites were reared on host plant leaves under controlled conditions at 18–25 °C, 60–80% relative humidity, and 15 : 9 h light : dark (L : D) for a few weeks, and subsequently maintained at 25 ± 1 °C. Each laboratory culture was initiated with more than 20 adult female mites. Forms of these mite populations were confirmed by male weapon morph (Saito, 1995; Sato *et al.*, 2013a). For phylogenetic analyses, we collected the closely related species, *S. longus* from Fukuoka (Fukuoka Prefecture, Japan) as the outgroup.

Cross-experiment

One population was selected in each area except for the HG + LW area. In this area, one HG and one LW population were selected. Females of selected populations were crossed with males from different populations in the same area (intra-area), other areas (interarea), same form (intraform) and other forms (interform). As controls, intrapopulation crosses and measurement of virgin oviposition were carried out in each selected population. In total, the numbers of pairs in the inter- and intrapopulation crosses were 722 (36 cross-combinations) and 122 (six cross-combinations), and the number of virgin females we observed in the virgin oviposition was 122 (six populations). Details of cross-combinations and the number of replicates in each are shown in Figs 2 and 3 and Table S4, and details of experiment procedures are as follows.

A piece of 1.0 × 3.0 cm was cut from a detached *M. sinensis* leaf and then placed on water-soaked cotton wool in a Petri dish. The cut edges were covered by thin strips of wet cotton wool. A female in the last moult before adulthood (teleiochrysalis stage) was collected from the mite culture and placed on the leaf arena. After the female moulted to the adult stage and constructed a nest, a male collected from the mite culture was introduced there. The female and male were allowed to mate and oviposit for 10 days and then they were removed from the leaf arena. In the virgin oviposition treatment, we carried out this procedure without male introduction. We excluded the pairs in which either the female or the male was found dead during the period of mating and oviposition (10 days) from analyses. We did not observe any bias in the mortality depending on cross-combination. Both the number of eggs and the offspring survival were assessed every 24 h. The daily check was continued until all offspring were confirmed to have matured or died. For unhatched eggs, the check was continued until they became apparently brown or deflated. The gender of offspring was checked after they moulted into adults. The cross-experiments were carried out under the same conditions as the mite rearings.

Whether or not females copulated with males from other populations (premating reproductive isolation) was checked by comparing the number of eggs with virgin oviposition, as the number of eggs laid by virgin females is significantly lower (Sato *et al.*, 2000a, b). Because males develop from unfertilized eggs, post-mating, prezygotic reproductive isolation was evaluated by comparing the ratio of male offspring to eggs (#sons/#eggs) from interpopulation crosses with that from intrapopulation crosses. Post-zygotic reproductive isolation was evaluated by comparing offspring mortality among diploid eggs [(#unhatched-eggs + #dead-juveniles)/(#eggs − #sons)]. We did not use offspring mortality among all eggs as the index of post-zygotic barrier as is done in studies on diploid organisms, because the

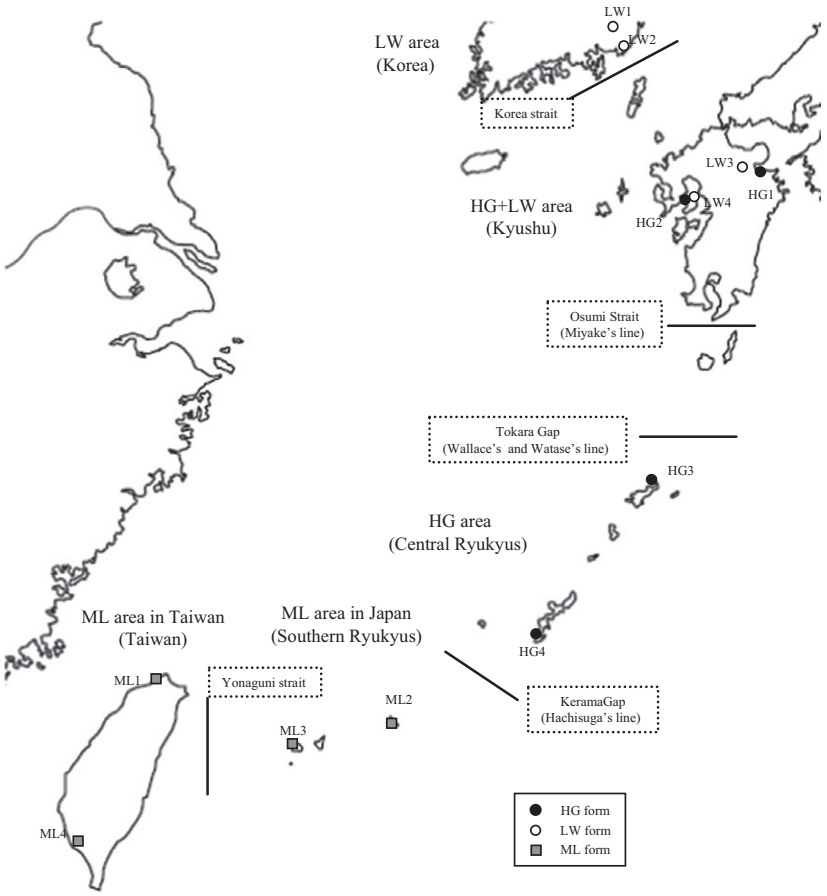

Fig. 1 Research area showing the locations from which *Stigmaeopsis miscanthi* was collected. Filled circles indicate populations of the high aggression (HG) form, open circles indicate populations of the low aggression (LW) form, and grey squares indicate populations of the mild aggression (ML) form (Y. Sato, Y. Tsuda, H. Sakamoto, M. Egas, T. Gotoh, Y. Saito, Y-X. Zhang, J-Z. Lin, J-T. Chao & A. Mochizuki, unpublished). These populations are grouped into five areas based on the current geographic distribution and are numbered in order of northern latitude in each form.

intensity of prezygotic reproductive barrier (fertilization rate) largely varied among cross-combinations, and the difference can strongly affect the offspring mortality among all eggs in haplodiploidy. For the calculation, we assessed the number of fertilized eggs as (#eggs − #sons) because offspring mortality for virgins is virtually zero (see Fig. 3; Table S4). We discarded data from replicates where the number of eggs was equal to the number of sons (#eggs − #sons = 0). Total reproductive isolation was evaluated by comparing values obtained by subtracting viable diploid offspring ratio from 1, [1 − (#daughters/#eggs)], from interpopulation crosses with the corresponding ratio from intrapopulation crosses.

DNA preparation and sequencing

In measures of genetic distance among populations and the phylogenetic analyses, we used the para-sodium channel gene of nuclear DNA (nDNA) and the cytochrome *c* oxidase subunit I gene (COI) of mtDNA. We used both nuclear and mitochondrial genes because in haplodiploid species mitochondrial genes are expected to introgress much faster than nuclear genes (Patten *et al.*, 2015). DNA was extracted from a single female mite from each population stored in 100% ethanol or acetone in a microtube using Wizard Genomic DNA Purification Kit (Promega, Madison, WI, USA), PrepMan Ultra Sample Preparation Reagent (Applied Biosystems, Foster City, CA, USA) or QIAamp DNA Micro Kit (Qiagen K. K., Tokyo, Japan). To amplify the fragment of para-sodium channel gene, polymerase chain reaction (PCR) was carried out using primers given in Table S1 in a 20-μL reaction mixture containing 1 μL of DNA sample, 2 μL of 10 × *Ex Taq* buffer (20 mM mg^{2+} plus; Takara Bio Inc., Otsu, Shiga, Japan), 0.2 μL of *TaKaRa Ex Taq* (5U μL^{-1}; Takara Bio Inc.), 1.6 μL of dNTP mix (2.5 mM each; Takara Bio Inc.), 1 μL of each primer (10 pmol μL^{-1} each) and 13.2 μL of ddH_2O. PCR cycling

(a) LW2 female (LW area)

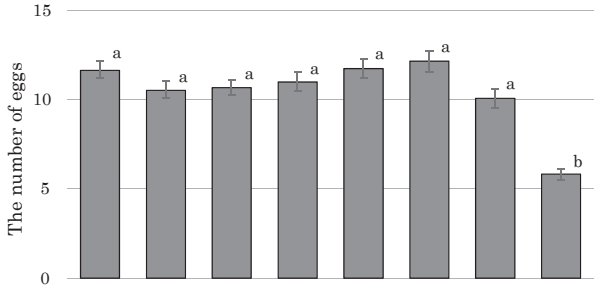

Male	LW2	LW1	LW4	HG2	HG4	ML3	ML4	–
Cross-type1	Intra population	Intraform		LW × HG		LW × ML		Virgin oviposition
Cross-type2		Intra area	Interarea					
No. of pairs	20	20	21	20	22	20	18	22

(b) LW4 female (HG + LW area)

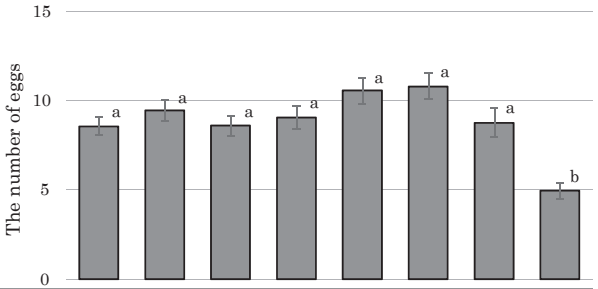

Male	LW4	LW3	LW2	HG2	HG4	ML3	ML4	–
Cross-type1	Intra population	Intraform		LW × HG		LW × ML		Virgin oviposition
Cross-type2		Intra area	Inter area	Intra area	Interarea			
No. of pairs	21	20	20	20	21	20	18	21

(c) HG4 female (HG area)

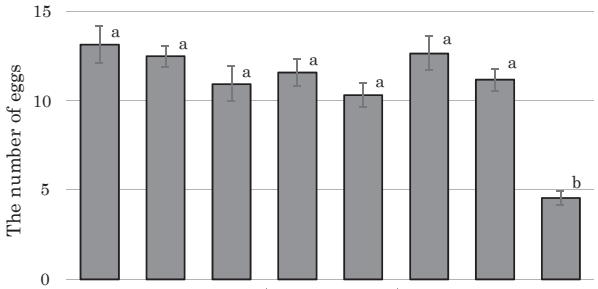

Male	HG4	HG3	HG2	LW2	LW4	ML3	ML4	–
Cross-type1	Intra population	Intraform		HG × LW		HG × ML		Virgin oviposition
Cross-type2		Intra area	Interarea					
No. of pairs	20	19	21	19	19	19	19	20

(d) HG2 female (HG + LW area)

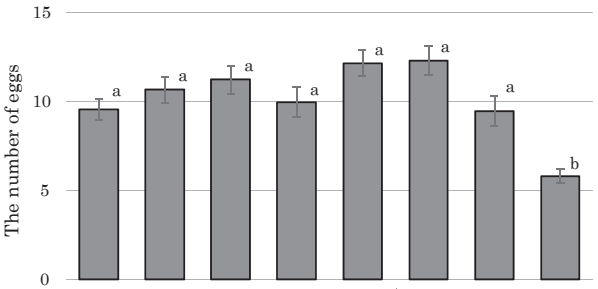

Male	HG2	HG1	HG4	LW4	LW2	ML3	ML4	–
Cross-type1	Intra population	Intraform		HG × LW		HG × ML		Virgin oviposition
Cross-type2		Intra area	Inter area	Intra area	Interarea			
No. of pairs	20	21	24	21	19	20	17	21

(e) ML3 female (ML area in Japan)

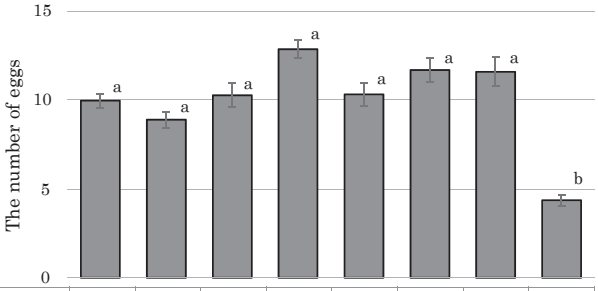

Male	ML3	ML2	ML4	LW2	LW4	HG2	HG4	–
Cross-type1	Intra population	Intraform		ML × LW		ML × HG		Virgin oviposition
Cross-type2		Intra area	Interarea					
No. of pairs	20	19	19	19	19	25	21	19

(f) ML4 female (ML area in Taiwan)

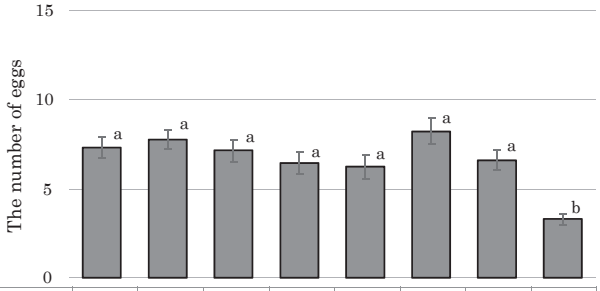

Male	ML4	ML1	ML3	LW2	LW4	HG2	HG4	–
Cross-type1	Intra population	Intraform		ML × LW		ML × HG		Virgin oviposition
Cross-type2		Intra area	Interarea					
No. of pairs	21	21	20	19	21	20	21	19

Fig. 2 The average number of eggs produced by females in intra- and interpopulation crosses and virgin females, for females from population LW2 (a), LW4 (b), HG4 (c), HG2 (d), ML3 (e) and ML4 (f). Column bars represent the means, and vertical line bars represent standard errors. Cross-type 1 and cross-type 2 indicate ecological and geographic classification of cross-combination, respectively. The number of eggs was compared with virgin oviposition in each female as an index of premating barrier, because the number of eggs laid by virgin females is significantly lower in *Stigmaeopsis miscanthi* (Sato *et al.*, 2000a, b). Different letters above column bars indicate statistically significant differences (Tukey's test for post hoc comparisons, $P < 0.05$).

conditions were 2 min at 94 °C, followed by 38 cycles of 30 s at 94 °C, 30 s at 53 °C and 1 min at 72 °C, and a final extension at 72 °C for 10 min. To amplify the fragment of mtCOI region, PCR was carried out using primers given in Table S1 (Matsuda *et al.*, 2014) in a 10-μL reaction mixture containing 1 μL of DNA sample, 1 μL of 10 × *Ex Taq* buffer (20 mM mg^{2+} plus; Takara Bio Inc.), 0.05 μL of *TaKaRa Ex Taq* (5U μL^{-1}, Takara Bio Inc.), 0.8 μL of dNTP mix (2.5 mM each; Takara Bio Inc.), 0.5 μL of each primer (10 pmol μL^{-1} each) and 6.35 μL of ddH_2O. PCR cycling conditions were 4 min at 94 °C, followed by 35 cycles of 1 min at 94 °C, 1 min at 45 °C and 1.5 min at 72 °C, and a final extension at 72 °C for 10 min. In some samples, the fragment was not amplified. Therefore, in the samples, PCR was carried out using primers that we designed (Table S1) in a 50-μL reaction mixture containing 1 μL of DNA sample, 25 μL of Premix Ex Taq (1.25 U/25 μL; Takara Bio Inc.) and 24 μL of ddH_2O, and PCR conditions were 1 min at 94 °C, followed by 35 cycles of 10 s at 98 °C, 30 s at 50 °C and 1 min at 72 °C without a final extension. PCR products were purified using QIAquick PCR Purification Kit (Qiagen) or ExoSAP-IT PCR Product Cleanup (Affymetrix, Inc., Cleveland, OH, USA), and the purified products were sequenced using ABI BigDye Terminator ver. 3, Cycle Sequencing Kit (Applied Biosystems) and ABI3130xl Genetic Analyzer (Applied Biosystems). A part of the samples was sequenced by an external service (FASMAC Co., Ltd., Atsugi, Kanagawa, Japan).

Phylogenetic analyses and genetic distance measurements

Obtained sequences of the para-sodium channel gene (GenBank accession numbers: MH015200–MH015213) and of the COI (GenBank accession numbers: MH029789–MH029801) were aligned using CLUSTAL W (codons) and CLUSTAL W (DNA), respectively (Thompson *et al.*, 1994), with default settings in MEGA6 (Tamura *et al.*, 2013). A maximum-likelihood (ML) tree of each region was constructed with MEGA 6 (Tamura *et al.*, 2013). As the substitution model for the ML trees, the Hasegawa–Kishino–Yano model was used with uniform rates for the para-sodium channel gene, and with nonuniform rates by assuming that a certain fraction of sites is evolutionarily invariable for the COI gene, according to the Bayesian information criteria in ML fits of 24 different nucleotide substitution models. Reliability of trees was evaluated by the bootstrap test ($N = 1000$).

Kimura 2-parameter genetic distances (Kimura, 1980) were calculated among the populations for each region using MEGA 6 (Tamura *et al.*, 2013), and the rate variation among sites was modelled with a gamma distribution (shape parameter = 1). As the phylogenetic relationships among the three forms were unclear in both ML trees (i.e. the bootstrap values supporting deep branches were low; Fig. S1), we did not consider their phylogenetic independence in the genetic distances as other papers did (Coyne & Orr, 1989, 1997; Sánchez-Guillén *et al.*, 2014). Moreover, previous results using 47 populations collected in the same geographic area show that para-sodium channel gene and COI genes are less diverse among populations from the same area and the same form than between different area and forms (Y. Sato, Y. Tsuda, H. Sakamoto, M. Egas, T. Gotoh, Y. Saito, Y-X. Zhang, J-Z. Lin, J-T. Chao & A. Mochizuki, unpublished). This suggests that intrapopulation diversity is very low and that one female sampled per population should be enough to represent the dominant genotype in the population.

Check for endosymbiont infections

To detect the presence of *Wolbachia*, *Cardinium* and *Spiroplasma* in the mites, we carried out PCR assay for these endosymbionts using primers given in Table S1 (Weisburg *et al.*, 1991; Zhou *et al.*, 1998; Fukatsu & Nikoh, 2000; Weeks *et al.*, 2003). Eight female mites were collected from each of the cultures of populations used in the cross-experiments in which reproductive barriers were detected (LW2, LW4, HG2, HG4, ML3 and ML4), and DNA was extracted from every single female mite in the same way as the previous experiment. PCR was carried out in a 10-μL reaction mixture containing 0.5 μL of DNA sample, 1 μL of 10 × *Ex Taq* buffer (20 mM Mg^{2+} plus, Takara Bio Inc.), 0.05 μL of *TaKaRa Ex Taq* (5U μL^{-1}; Takara Bio Inc.), 0.8 μL of dNTP mix (2.5 mM each; Takara Bio Inc.), 0.5 μL of each primer (10 pmol μL^{-1} each) and 6.65 μL of ddH_2O. PCR cycling conditions were 2 min at 94 °C, followed by 35 cycles of 30 s at 94 °C, 30 s at 55 °C and 1 min at 72 °C, and a final extension at 72 °C for 10 min. As positive controls, we used the DNA sample of *Tetranychus truncatus* in the detection of *Wolbachia* and *Spiroplasma* infections and that of *T. parakanzawai* in the detection *Cardinium* infection. As a negative control, we added ddH_2O instead of DNA sample. We checked whether DNA extraction had not failed in tested *S. miscanthi* samples by amplifying a fragment of 28S rDNA

(a) LW2 female (LW area)

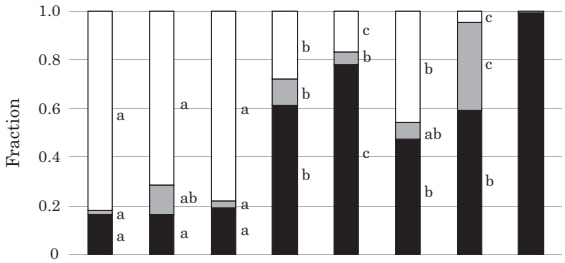

Male	LW2	LW1	LW4	HG2	HG4	ML3	ML4	–
Cross-type1	Intra population	Intraform		LW × HG		LW × ML		Virgin oviposition
Cross-type2		Intra area	Interarea					
No. of pairs	20	20	21	20	22	20	18	22

(b) LW4 female (HG + LW area)

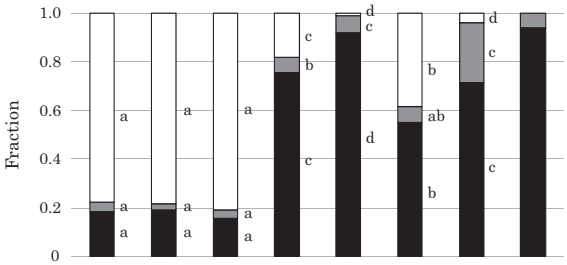

Male	LW4	LW3	LW2	HG2	HG4	ML3	ML4	–
Cross-type1	Intra population	Intraform		LW × HG		LW × ML		Virgin oviposition
Cross-type2		Intra area	Inter area	Intra area	Interarea			
No. of pairs	21	20	20	20	21	20	18	21

(c) HG4 female (HG area)

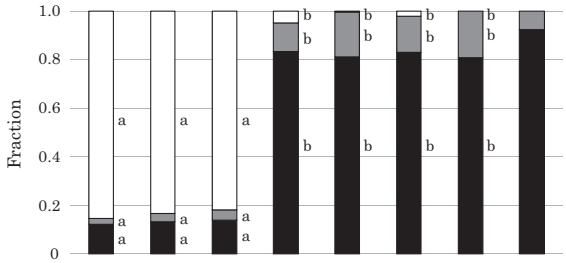

Male	HG4	HG3	HG2	LW2	LW4	ML3	ML4	–
Cross-type1	Intra population	Intraform		HG × LW		HG × ML		Virgin oviposition
Cross-type2		Intra area	Interarea					
No. of pairs	20	19	21	19	19	19	19	20

(d) HG2 female (HG + LW area)

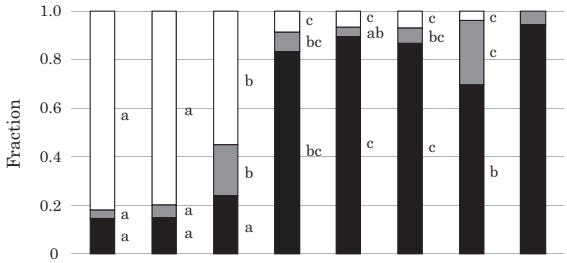

Male	HG2	HG1	HG4	LW4	LW2	ML3	ML4	–
Cross-type1	Intra population	Intraform		HG × LW		HG × ML		Virgin oviposition
Cross-type2		Intra area	Inter area	Intra area	Interarea			
No. of pairs	20	21	24	21	19	20	17	21

(e) ML3 female (ML area in Japan)

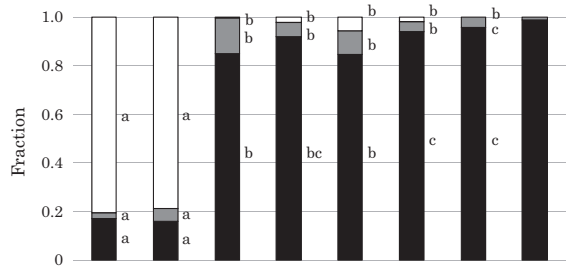

Male	ML3	ML2	ML4	LW2	LW4	HG2	HG4	–
Cross-type1	Intra population	Intraform		ML × LW		ML × HG		Virgin oviposition
Cross-type2		Intra area	Interarea					

(f) ML4 female (ML area in Taiwan)

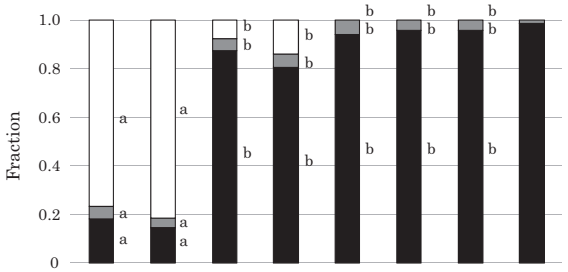

Male	ML4	ML1	ML3	LW2	LW4	HG2	HG4	–
Cross-type1	Intra population	Intraform		ML × LW		ML × HG		Virgin oviposition
Cross-type2		Intra area	Interarea					

Fig. 3 Relative proportions of sons, dead offspring (dead juveniles and unhatched eggs) and daughters to eggs produced by females in intra- and interpopulation crosses and virgin females, for females from population LW2 (a), LW4 (b), HG4 (c), HG2 (d), ML3 (e) and ML4 (f). The plots show the ratios calculated in each cross-combination; however, statistical analyses were performed using the ratios in each pair. Male offspring ratio to eggs (#sons/#eggs), dead offspring ratio to diploid eggs [# dead offspring/(#eggs − #sons)] and values obtained by subtracting female offspring ratio from 1 [1 − (#daughter/#eggs)] were compared among cross-combinations (excluding virgin oviposition) in each female population as indexes of prezygotic barrier, post-zygotic barrier and total reproductive barrier (for details, see the text). Letters on the right side of bars show the results of statistical analyses (lower letters: prezygotic barrier, middle letters: post-zygotic barrier, upper letters: total reproductive barrier), and different letters indicate statistically significant differences (Tukey's test for post hoc comparisons, $P < 0.05$).

using a pair of primers given in Table S1 (Hillis & Dixon, 1991). PCR was carried out in a 10-μL reaction mixture containing 0.5 μL of DNA sample, 2 μL of 5 × KAPA buffer (without Mg^{2+}; Kapa Biosystems, Boston, MA, USA), 0.05 μL of KAPATaq EXtra (5U μL^{-1}; Kapa Biosystems), 0.7 μL of $MgCl^2$ (25 mM; Kapa Biosystems), 0.3 μL of dNTP mix (10 mM each; Kapa Biosystems), 0.5 μL of each primer (10 pmol μL^{-1} each) and 5.45 μL of ddH_2O. PCR cycling conditions were 4 min at 94 °C, followed by 35 cycles of 1 min at 94 °C, 1 min at 52 °C, and 3 min at 72 °C and a final extension at 72 °C for 5 min.

Statistical analyses

Analyses were carried out with the statistical package R version 3.2.0 (R Core Team, 2015). To check for premating barriers, we analysed the number of eggs laid by females from each population used in the crossing experiments (hereafter, we refer to the source population of such females as 'female population') using a Poisson generalized linear model (Poisson GLM) with cross-combination and using Tukey's test for post hoc comparisons (Hothorn *et al.*, 2008). Overdispersion, complete separation or quasi-complete separation was not detected in the analyses. To check for post-mating, prezygotic barriers, post-zygotic barriers and total reproductive barriers, male offspring ratio to eggs, offspring mortality among diploid eggs and the value obtained by subtracting viable diploid offspring ratio from 1 were analysed in each female population using binomial generalized linear models (binomial GLMs) with cross-combination and using Tukey's test for post hoc comparisons (Hothorn *et al.*, 2008). When we detected overdispersion in these models, we applied a quasibinomial distribution as an error distribution. When we detected a complete separation or quasi-complete separation, we applied a binomial-response GLM using the bias reduction method developed in (Firth, 1993) (*brglm* in the package, *brglm*; Kosmidis, 2013).

To determine the relationships of post-mating, prezygotic barrier, post-zygotic barrier and total reproductive barrier with genetic distance, we analysed the effects of genetic distance, female population and their interaction on male offspring ratio to eggs, offspring mortality among diploid eggs and the value obtained by subtracting viable diploid offspring ratio from 1 with quasibinomial GLMs to account for overdispersion. The time course for the evolution of reproductive isolation was analysed by the slope of regression line of reproductive isolation intensity on genetic distance. To compare the slope among different types of reproductive barriers, we constructed a quasibinomial GLM with genetic distance in each type of reproductive barrier, and using the model, we estimated the genetic distance for which the barriers become nearly complete (99% and 99.9% barrier). To compare the slope of prezygotic reproductive isolation between allopatric and parapatric populations, we constructed a quasibinomial GLM with genetic distance, geographic relationship, female form and the interactions using the data set of HG and LW females.

Results

Premating barrier

In all interpopulation crosses, the number of eggs was significantly larger than those produced by virgins, and similar to those produced in intrapopulation crosses (Poisson GLMs; LW2: $\chi^2_7 = 66.272$, $P < 0.001$; LW4: $\chi^2_7 = 58.804$, $P < 0.001$; HG2: $\chi^2_7 = 66.472$, $P < 0.001$; HG4: $\chi^2_7 = 114.90$, $P < 0.001$; ML3: $\chi^2_7 = 104.88$, $P < 0.001$; ML4: $\chi^2_7 = 52.651$, $P < 0.001$; Fig. 2; Table S4), indicating that mating occurred regardless of cross-combination. The number of eggs was not significantly different between inter- and intrapopulation crosses (Fig. 2; Table S4).

Post-mating, prezygotic barrier

The ratio of male offspring to eggs, which we use as an index of post-mating, prezygotic barrier intensity, was significantly different among cross-combinations in each female population (quasibinomial GLMs; LW2: $F_{6,126} = 40.769$, $P < 0.001$; LW4: $F_{6,133} = 71.984$, $P < 0.001$; HG2: $F_{6,135} = 67.191$, $P < 0.001$; HG4: $F_{6,129} = 72.494$, $P < 0.001$; ML3: $F_{6,135} = 195.24$, $P < 0.001$; ML4: $F_{6,136} = 49.178$, $P < 0.001$; Fig. 3; Table S4). In LW and HG populations, such post-mating, prezygotic barriers were exclusively detected in the crosses with males from other forms (Fig. 3; Table S4).

In ML females, the barriers were detected not only in the crosses with males from other forms but also in the crosses with allopatric ML males (Fig. 3; Table S4). Asymmetries in prezygotic reproductive barrier were found; LW females tended to produce more daughters (i.e. hybrid offspring) than HG and ML females in reciprocal interform crosses (Fig. 3; Table S4). Genetic distance based on nDNA (see Table S2) and mtDNA (see Table S3) explained the intensity of post-mating, prezygotic reproductive barrier (nDNA: $t_{30} = 2.08$, $P < 0.05$; $t_{30} = 5.962$, mtDNA: $P < 0.001$; Fig. 4; Table S5). The slope of regression line of reproductive barrier intensity on genetic distance was significantly different among female populations in the analysis based on mtDNA sequences; the slopes in HG4, ML4 and ML3 female populations were significantly steeper than that in LW2 female populations (HG4 slope vs. LW2 slope: $t_{30} = 2.991$, $P < 0.01$; ML4 slope vs. LW2 slope: $t_{30} = 3.047$, $P < 0.01$; ML3 slope vs. LW2 slope: $t_{30} = 3.519$, $P < 0.01$; Fig. 4; Table S5). However, such significant difference based on mtDNA sequences was not detected for HG2 and LW4 populations, and for all populations based on nDNA sequences (Fig. 4; see Table S5 for all statistical results). The slope of regression line in LW females from the parapatric area (LW4) seemed to be steeper than in LW females from the allopatric area (LW2); however, the difference was not significant (Fig. 4; Tables S5 and S6). In HG females, such tendency was not found (Fig. 4; Tables S5 and S6).

Post-zygotic barrier

Offspring mortality among diploid eggs, which we use as an index of post-zygotic barrier intensity, was significantly different among cross-combinations in each female population (binomial or quasibinomial GLMs; LW2: $F_{6,126} = 25.091$, $P < 0.001$; LW4: $\chi^2_6 = 223.17$, $P < 0.001$; HG2: $F_{6,110} = 12.772$, $P < 0.001$; HG4: $\chi^2_6 = 513.22$, $P < 0.001$; ML3: $\chi^2_6 = 249.49$, $P < 0.001$, ML4: $\chi^2_6 = 83.576$, $P < 0.001$; Fig. 3; Table S4). In LW and HG females, offspring mortality among diploid eggs was significantly higher in the interform crosses compared to the intraform crosses (Fig. 3; Table S4). However, in ML females, offspring mortality among diploid eggs was significantly higher not only in the interform crosses but also in the crosses with allopatric ML males compared to the intraform crosses (Fig. 3; Table S4). Asymmetries in reproductive incompatibility among the reciprocal combinations were found; offspring mortality tended to be strong in the crosses with ML4 males (Fig. 3; Table S4). Genetic distance based on nDNA (see Table S2) and mtDNA (see Table S3) explained the intensity of post-zygotic reproductive barrier (nDNA: $t_{30} = 2.48$, $P < 0.05$; mtDNA: $t_{30} = 2.76$ $P < 0.01$; Fig. 4; Table S5). The slope of regression line of reproductive barrier intensity on genetic distance was significantly different among female populations in both of nDNA and mtDNA; the slope in HG4 was significantly steeper than that in ML4 based on nDNA ($t_{30} = 2.71$, $P < 0.05$; Fig. 4; Table S5), and the slope in HG4 was significantly steeper than that in LW2 based on mtDNA ($t_{30} = 2.27$, $P < 0.05$; Fig. 4; Table S5). Such significant difference was not detected for LW2, LW4, HG2 and ML3 populations based on nDNA and for LW4, HG2, ML3 and ML4 populations based on mtDNA (Fig. 4; see Table S5 for all statistical results).

Total reproductive barrier

The value obtained by subtracting viable diploid offspring ratio from 1, our index of total reproductive barrier, was significantly different among cross-combinations in each female population (binomial or quasibinomial GLMs; LW2: $F_{6,134} = 41.623$, $P < 0.001$; LW4: $\chi^2_6 = 701.49$, $P < 0.001$; HG2: $F_{6,135} = 42.843$, $P < 0.001$; $\chi^2_6 = 1317.100$, $P < 0.001$; ML3: $\chi^2_6 = 965.35$, $P < 0.001$; ML4: $F_{6,136} = 61.693$, $P < 0.001$; Fig. 3; Table S4). In LW and HG females, a reproductive barrier was detected in all crosses involving males from one of the other forms (Fig. 3; Table S4). However, in ML females, the ratio of male and dead offspring to eggs was significantly higher not only in the interform crosses but also in the crosses with allopatric ML males compared to the intraform crosses (Fig. 3; Table S4). Genetic distance based on nDNA (see Table S2) and mtDNA (see Table S3) explained the intensity of total reproductive barrier (nDNA: $t_{30} = 3.32$, $P < 0.01$; mtDNA: $t_{30} = 4.98$, $P < 0.001$; Fig. 4; Table S5). The slope of reproductive barrier intensity on genetic distance was significantly different among female populations both in nDNA and mtDNA; the slopes in ML3 and HG4 were significantly steeper than that in LW2 based on nDNA (ML3 slope vs. LW2 slope: $t_{30} = 2.09$, $P < 0.05$; HG4 slope vs. LW2 slope: $t_{30} = 2.65$, $P < 0.05$; Fig. 4; Table S5), and those in ML3, HG4 and ML4 were significantly steeper than that in LW2 in mtDNA (ML4 slope vs. LW2 slope: $t_{30} = 2.22$, $P < 0.05$; ML3 slope vs. LW2 slope: $t_{30} = 2.84$, $P < 0.01$; HG4 slope vs. LW2 slope: $t_{30} = 3.01$, $P < 0.01$; Fig. 4; Table S5). Such significant difference was not detected for LW4, ML4 and HG2 populations based on nDNA and for LW4 and HG2 populations based on mtDNA (Fig. 4; see Table S5 for all statistical results).

Genetic distance for which reproductive barrier is nearly complete

Post-mating, prezygotic barrier was estimated to be nearly complete at genetic distances of 0.022–0.031 and 0.190–0.258 (99.0–99.9% barrier) based on the nDNA marker and mtDNA marker, respectively (Table 1). The models estimated that nearly complete post-zygotic barrier appears at genetic distances of 0.026–0.034 and 0.240–0.314 (99.0–99.9% barrier)

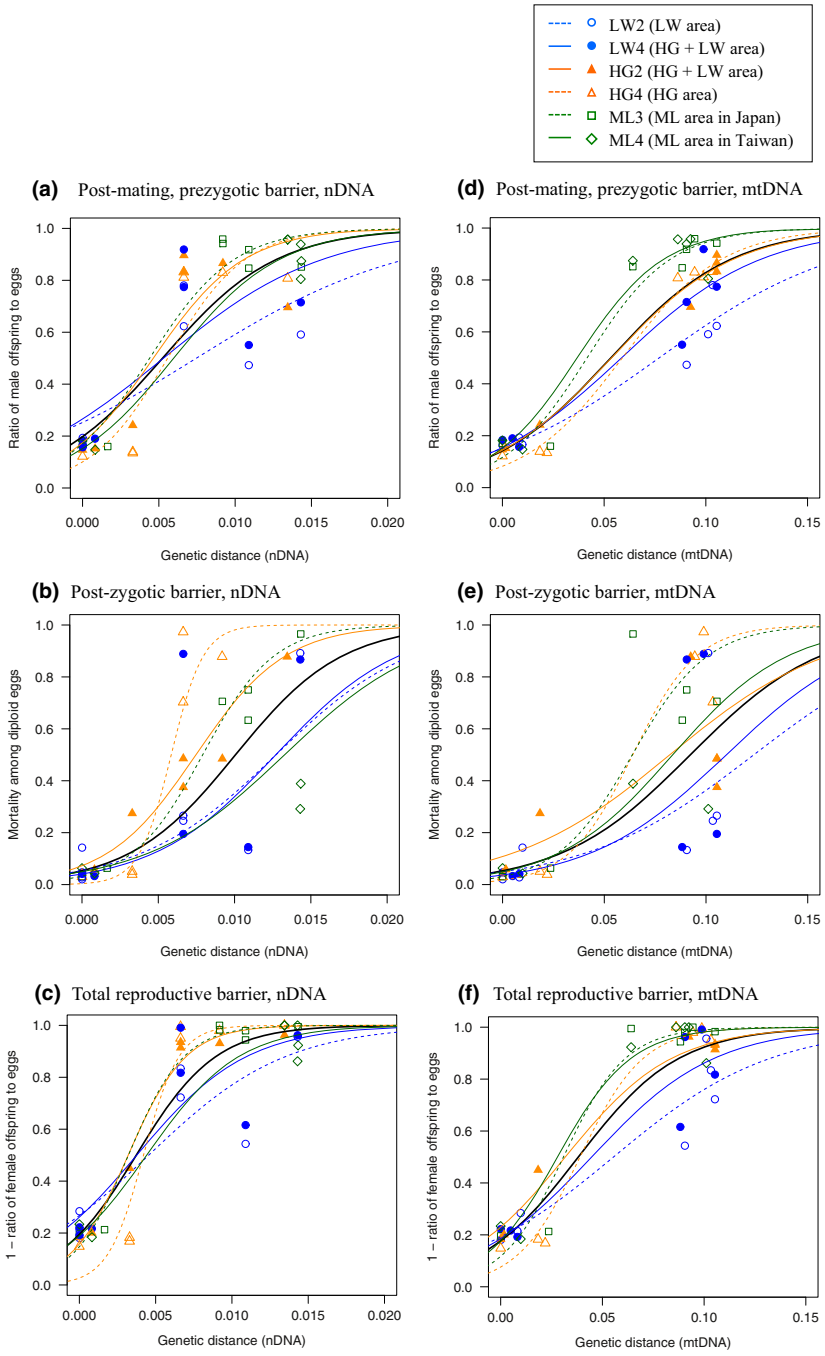

Fig. 4 Relationship between reproductive barrier and genetic distance calculated by Kimura's 2-parameter model in each stage: premating, prezygotic barrier (a), post-zygotic barrier (b) and total reproductive barrier (c) in nDNA (para-sodium channel gene) and those (d, e and f) in mtDNA (COI). Blue open circles show crosses in which the female is of LW2 from LW area (allopatric area), orange open triangles show crosses in which the female is of HG4 from HG area (allopatric area), and green open squares show the crosses in which the females are of ML3 and ML4 from ML areas in Japan and Taiwan (allopatric area). Circles filled with blue and orange show the crosses in which the females are of LW4 and HG 2 from HG + LW area (parapatric area), respectively. Coloured lines show the model prediction of the relationship between reproductive barrier and genetic distance in each female population, and the black bold line shows the model prediction for all female populations together.

Table 1 Quasibinomial generalized linear models of post-mating, prezygotic barrier (A), post-zygotic barrier (B) and total reproductive barrier (C) with genetic distances based on nDNA (para-sodium channel gene) and mtDNA (COI), and estimated genetic distance for which reproductive barriers would appear 99% and 99.9%.

	Quasibinomial GLM				Estimated genetic distance	
Explanatory variable	Estimate	SE	*t* value	*P*	99% barrier	99.9% barrier
(A) Prezygotic barrier						
nDNA						
(Intercept)	−1.402	0.266	−5.271	< 0.001	0.022	0.031
Genetic distance	267.445	36.578	7.312	< 0.001		
mtDNA						
(Intercept)	−1.800	0.212	−8.478	< 0.001	0.190	0.258
Genetic distance	33.735	2.835	11.901	< 0.001		
(B) Post-zygotic barrier						
nDNA						
(Intercept)	−2.876	0.305	−9.420	< 0.001	0.026	0.034
Genetic distance	285.772	38.802	7.365	< 0.001		
mtDNA						
(Intercept)	−2.882	0.334	−8.628	< 0.001	0.240	0.314
Genetic distance	31.206	4.536	6.880	< 0.001		
(C) Total reproductive barrier						
nDNA						
(Intercept)	−1.422	0.298	−4.768	< 0.001	0.016	0.022
Genetic distance	381.456	51.795	7.365	< 0.001		
mtDNA						
(Intercept)	−1.539	0.243	−6.326	< 0.001	0.152	0.210
Genetic distance	40.299	3.938	10.233	< 0.001		

mtDNA, mitochondrial DNA; nDNA, nuclear DNA.

based on the nDNA marker and mtDNA marker, respectively (Table 1). The models estimated that total reproductive barrier appears at genetic distances of 0.016–0.022 and 0.152–0.210 (99.0–99.9% barrier) based on the nDNA marker and mtDNA marker, respectively (Table 1).

Endosymbiont infections

Wolbachia infection was detected in one of eight ML4 females, representing 12.5% infection prevalence (Fig. S2). *Cardinium* infection was not detected in any females (Fig. S3). *Spiroplasma* infection was detected in one of eight HG2 females, one of eight ML3 females and one of eight ML4 females (12.5% infection prevalence in each population; Fig. S4). DNA extraction was confirmed in all tested samples (Fig. S5).

Discussion

In this study, we tested whether intensity of reproductive isolation increases with genetic distance and whether biogeographic patterns (allopatry/parapatry) affect the evolution of prezygotic reproductive barriers in the social spider mite, *S. miscanthi*. We found that a strong but incomplete post-mating reproductive barrier exists between allopatric populations of HG and LW forms, as is the case between parapatric populations (Sato *et al.*, 2000a, b). In addition, we found that the ML form, which was recently found and occurs in more subtropical areas (Y. Sato, Y. Tsuda, H. Sakamoto, M. Egas, T. Gotoh, Y. Saito, Y-X. Zhang, J-Z. Lin, J-T. Chao & A. Mochizuki, unpublished), is reproductively isolated from both HG and LW forms. Additionally, the allopatric populations of the ML form we tested (i.e. in Taiwan and Japan) are also reproductively isolated. As in previous studies (Sato *et al.*, 2000a, 2008), the post-mating, prezygotic barrier largely contributed to the total reproductive barrier in the mite (on average 81%, with a range of 48–97%). Regarding reinforcement of prezygotic isolation among parapatric populations, we found a tendency that reproductive isolation evolves faster in LW females from parapatric areas than those from allopatric areas. Taken together, these results support the prevalent view that reproductive barriers evolve gradually as a by-product of genetic changes accumulated by natural selection and genetic drift, whereas groups are segregated spatially or temporally (Futuyma, 1998; Howard & Berlocher, 1998; Coyne & Orr, 2004).

We also found asymmetries in reproductive incompatibility among the reciprocal combinations (Fig. 3; Table S4). Asymmetric cytoplasmic incompatibility is often caused by endosymbiont infections (e.g. Werren *et al.*, 2008) and has been shown for *Wolbachia* and *Cardinium* infection in spider mites (Gotoh *et al.*, 2005,

2007; Ros & Breeuwer, 2009; Zhu *et al.*, 2012). Infections of *Wolbachia* and *Spiroplasma* were detected at low frequency in HG and ML form populations (12.5% infection prevalence of *Wolbachia* in ML4 and 12.5% infection prevalence of *Spiroplasma* in HG4, ML3 and ML4). Offspring mortality tended to be strong in the crosses with ML4 males (Fig. 3; Table S4). As *Wolbachia*-infected males generally disturb reproduction of uninfected females (e.g. Werren *et al.*, 2008), *Wolbachia* infection might be responsible, at least partially, of the asymmetries observed in post-zygotic reproductive barrier among the reciprocal combinations. Conversely, such tendency was not observed in crosses involving HG2 and ML3 males, whereas the prevalence of *Spiroplasma* was found to be c.a. 12.5% in these populations. Although this endosymbiont has been previously reported in spider mites (Zhang *et al.*, 2016; Staudacher *et al.*, 2017), its effects on spider mite reproduction are, to our knowledge, still unknown and our results suggest that it does not induce cytoplasmic incompatibility in our system. Note, however, that our sample size for endosymbiont detection is low (eight females per population) and a more extensive assessment of endosymbiont prevalence (including other reproductive manipulators found in the Acari, such as *Rickettsia* and *Arsenophonus*; Hoy & Jeyaprakash, 2005; Clay *et al.*, 2008; Dergousoff & Chilton, 2010; Clayton *et al.*, 2015; Zhang *et al.*, 2016; Duron *et al.*, 2017), along with a full characterization of their effects in our populations would allow to determine their potential role in the incompatibilities observed here. Asymmetries in prezygotic reproductive barrier were also found; LW females tended to produce more daughters (i.e. hybrid offspring) than HG and ML females in reciprocal interform crosses (Fig. 3; Table S4). The pattern is in disagreement with known incompatibility effects of these endosymbionts, as endosymbiont infections were not detected in LW populations but in HG and ML populations. Except for endosymbiont infections, several mechanisms possibly cause the asymmetric post-mating incompatibilities; HG and ML females might fail to store sperm from different forms after mating, sperm from LW males might fail to reach the site of fertilization inside bodies of females from other forms, and sperm from LW males might fail to fertilize eggs (e.g. Rose *et al.*, 2014). Otherwise, embryos from fertilized eggs of HG and ML females might fail to develop because of negative cyto-nuclear interactions, that is between mitochondrial genes of the HG and ML forms and nuclear genes of the LW form (e.g. Hill, 2015). To address which mechanisms cause the asymmetric post-mating, prezygotic incompatibilities, physiological and cytological investigations would be necessary.

In this study, we did not include hybrid sterility in evaluation of post-zygotic barriers. Generally, hybrid sterility evolves faster than hybrid inviability (Coyne & Orr, 2004). The scale of the molecular clock largely depends on DNA (nuclear or mitochondrial) and markers (e.g. Sánchez-Guillén *et al.*, 2014), and genetic distance would be different depending on models used in the estimation even if their divergence time is the same. However, the mites used in this study are quite young groups which have been diverging recently, as the ranges of genetic distance are 0–0.105 in mtDNA (COI) and 0–0.014 in nDNA (para-sodium channel gene), where those ranges in previous studies are 0–2.0 in *Drosophila* (calculated by Nei's genetic distance and allozyme; Coyne & Orr, 1989, 1997), 0–1.2 in Lepidoptera (calculated by Nei's genetic distance and allozyme and/or other several genes; Presgraves, 2002), and 0–0.60 in damselflies (calculated by Kimura 2-parameter distance and mtDNA COII (−0.009 to 0.280), mtDNA CYTB (−0.001 to 0.179) and nDNA 18S–28S (0–0.540); Sánchez-Guillén *et al.*, 2014). Also, the total reproductive barrier estimated in the interform crosses is so high that few hybrid daughters were produced (see Fig. 3 and Table S4). Hybrid sterility may contribute to the reproductive barriers among the forms, but this does not affect our conclusion that post-mating, prezygotic barriers contribute most to reproductive isolation. By including hybrid sterility in future studies, the relationship with genetic distance might become clearer, and insight may be gained in genetic incompatibilities (cf. Knegt *et al.*, 2017).

It is generally expected that prezygotic barriers evolve faster among parapatric populations than among allopatric ones, by assuming reinforcement of this reproductive barrier in the contact zone (Butlin, 1995; Futuyma, 1998; Howard & Berlocher, 1998; Coyne & Orr, 2004; Lukhtanov *et al.*, 2005; Pfennig & Rice, 2014). In LW females, the post-mating, prezygotic barrier when cross-mated with HG males seemed stronger among populations from the parapatric area than among those from the allopatric area, although this difference was not significant. However, such tendency was not observed in HG females cross-mated with LW males. These differences appear in line with ecological and behavioural relationships between HG and LW forms. The females construct woven nests, and both types of males enter the nests regardless of the type of the female who constructed the nest (Sato *et al.*, 2015). Males easily fight with other males and kill each other for ownership of nests, and HG males tend to win against LW males in any nest (Sato *et al.*, 2013b). In addition, HG males show higher activity in mating behaviour towards both HG and LW females, compared to LW males (Sato *et al.*, 2015). Together, this suggests that LW females suffer reproductive interference by HG males in their contact zone, whereas HG females are protected from reproductive interference by strong, aggressive and active HG males. Assuming that hybridization is maladaptive, then, LW females in parapatric populations may be under stronger selection

for prezygotic isolation than LW females in allopatric populations, but HG females may not. As a next step, it might be worth to test the prediction again in LW females by increasing the number of LW form populations in the analyses of regression line of prezygotic barrier intensity on genetic distance, and also by revealing mechanisms to control fertilization. Studies addressing the male perspective are also necessary, for example, by conducting male mate choice experiments.

As far as we know, our study is the first comparative study on reproductive barriers and genetic distance in haplodiploid animals. Testing theory in various genetic systems is important for confirming its generality. In addition, each genetic system may have different strengths for this kind of study. In haplodiploid animals, females and males develop from fertilized and unfertilized eggs, respectively, and – as our study illustrates – pre- and post-zygotic reproductive barriers can be easily inferred from sex ratio and mortality in the offspring. In studies on diploid animals, post-mating prezygotic barriers are referred to as cryptic reproductive isolation to include problems with sperm transfer during copulation (e.g. Price *et al.*, 2001; Chang, 2004; Nosil & Crespi, 2006; Matute, 2010). The use of haplodiploid animals may facilitate the study of this reproductive barrier, because it can be directly inferred from a male bias in offspring sex ratio of mated females (although for species with functional haplodiploidy (Herrick & Seger, 1999), the possibility of parental genome elimination after fertilization should be taken into account as post-zygotic barrier rather than prezygotic barrier). Another strength of haplodiploid animals lies in analysing hybrid incompatibility. By analysing hybrid haploid males from two partially incompatible strains of a haplodiploid mite species, Knegt *et al.* (2017) tested the Bateson–Dobzhansky–Muller model, which emphasizes epistatic interactions between alleles to explain hybrid breakdown, without suffering from the effects of dominance-recessivity hiding epistatic interactions between loci. Also, in some haplodiploid species, it is possible to generate sex-reversed diploid males to unravel dominance and dosage effects in hybrid incompatibility (Beukeboom *et al.*, 2015). Therefore, haplodiploid animals are promising material in the study of evolutionary mechanisms underlying reproductive isolation.

Acknowledgments

We thank Dr Johannes A. J. Breeuwer at University of Amsterdam in the Netherlands for his valuable comments and advice to this study. We thank reviewers for their valuable comments and suggestions on our manuscript. We thank Dr Suguru Ohno at Okinawa Prefectural Agricultural Research Center in Japan for his help in *S. miscanthi* collections in the mainland of Okinawa Prefecture and in Miyako Island. We also thank Drs Kwang-Youl Seol and Siwoo Lee at Rural Development Administration in Republic of Korea for their help in *S. miscanthi* collections in South Korea. *S. miscanthi* collected from Korea and Taiwan were brought and reared with permission from the Ministry of Agriculture, Forestry, and Fisheries, Japan (permission number: 21-115). This study was mainly supported by JSPS KAKENHI Grant Numbers JP09J01045 (YS), JP26891003 (YS). This study was also supported in part by JSPS KAKENHI Grant Numbers JP25292033 (TG), JP17K07556 (YS).

References

Beukeboom, L.W., Koevoets, T., Morales, H.E., Ferber, S. & van de Zande, L. 2015. Hybrid incompatibilities are affected by dominance and dosage in the haplodiploid wasp *Nasonia*. *Front. Genet.* **6**: 140.

Butlin, R.K. 1995. Reinforcement: an idea evolving. *Trends Ecol. Evol.* **10**: 432–434.

Chang, A.S. 2004. Conspecific sperm precedence in sister species of *Drosophila* with overlapping ranges. *Evolution* **58**: 781–789.

Clay, K., Klyachko, O., Grindle, N., Civitello, D., Oleske, D. & Fuqua, C. 2008. Microbial communities and interactions in the lone star tick, *Amblyomma americanum*. *Mol. Ecol.* **17**: 4371–4381.

Clayton, K.A., Gall, C.A., Mason, K.L., Scoles, G.A. & Brayton, K.A. 2015. The characterization and manipulation of the bacterial microbiome of the Rocky Mountain wood tick, *Dermacentor andersoni*. *Parasit. Vectors* **8**: 632.

Clemente, S.H., Rodrigues, L.R., Ponce, R., Varela, S.A.M. & Magalhães, S. 2016. Incomplete species recognition entails few costs in spider mites, despite first-male precedence. *Behav. Ecol. Sociobiol.* **70**: 1161–1170.

Coyne, J.A. & Orr, H.A. 1989. Patterns of speciation in *Drosophila*. *Evolution* **43**: 362–381.

Coyne, J.A. & Orr, H.A. 1997. "Patterns of speciation in *Drosophila*" revisited. *Evolution* **51**: 295–303.

Coyne, J.A. & Orr, H.A. 2004. *Speciation*, 1st edn. Sinauer Associates Inc, Sunderland, MA.

Dergousoff, S.J. & Chilton, N.B. 2010. Detection of a new *Arsenophonus*-type bacterium in Canadian populations of the Rocky Mountain wood tick, *Dermacentor andersoni*. *Exp. Appl. Acarol.* **52**: 85–91.

Duron, O., Binetruy, F., Noël, V., Cremaschi, J., McCoy, K.D., Arnathau, C. *et al.* 2017. Evolutionary changes in symbiont community structure in ticks. *Mol. Ecol.* **26**: 2905–2921.

Firth, D. 1993. Bias reduction of maximum likelihood estimates. *Biometrika* **80**: 27–38.

Fukatsu, T. & Nikoh, N. 2000. Endosymbiotic microbiota of the bamboo pseudococcid *Antonina crawii* (Insecta, Homoptera). *Appl. Environ. Microbiol.* **66**: 643–650.

Futuyma, D.J. 1998. *Evolutionary Biology*, 3rd edn. Sinauer Associates Inc, Sunderland, MA.

Gotoh, T. 1986. Reproductive isolation between the two forms of *Panonychus akitanus* Ehara (Acarina: Tetranychidae). *Exp. Appl. Acarol.* **2**: 153–160.

Gotoh, T. & Noguchi, O. 1990. Developmental success and reproductive incompatibility among populations of the

European red mite, *Panonychus ulmi* (Acari: Tetranychidae). *Exp. Appl. Acarol.* **10**: 157–165.

Gotoh, T. & Takayama, K. 1992. Developmental characteristics, genetic compatibility and esterase zymograms in three strains of the hawthorn spider mite, *Tetranychus viennensis* Zacher (Acari: Tetranychidae). *J. Acarol. Soc. Jpn* **1**: 45–60.

Gotoh, T., Abe, T., Kurihara, A. & Suzuki, M. 1995. Genetic incompatibility in local populations of the spider mite, *Tetranychus quercivorus* Ehara et Gotoh (Acari: Tetranychidae). *Appl. Entomol. Zool.* **30**: 361–368.

Gotoh, T., Noda, H., Fujita, T., Iwadate, K., Higo, Y., Saito, S. *et al.* 2005. *Wolbachia* and nuclear–nuclear interactions contribute to reproductive incompatibility in the spider mite *Panonychus mori* (Acari: Tetranychidae). *Heredity* **94**: 237–246.

Gotoh, T., Noda, H. & Ito, S. 2007. *Cardinium* symbionts cause cytoplasmic incompatibility in spider mites. *Heredity* **98**: 13–20.

Gotoh, T., Araki, R., Boubou, A., Migeon, A., Ferragut, F. & Navajas, M. 2009. Evidence of co-specificity between *Tetranychus evansi* and *Tetranychus takafujii* (Acari: Prostigmata, Tetranychidae): comments on taxonomic and agricultural aspects. *Int. J. Acarol.* **35**: 485–501.

Herrick, G. & Seger, J. 1999. Imprinting and paternal genome elimination in insects. In: *Genomic Imprinting. Results and Problems in Cell Differentiation* (R. Ohlsson, ed.), vol. **25**, pp. 41–71. Springer, Berlin, Heidelberg.

Hill, G.E. 2015. Mitonuclear ecology. *Mol. Biol. Evol.* **32**: 1917–1927.

Hillis, D.M. & Dixon, M.T. 1991. Ribosomal DNA: molecular evolution and phylogenetic inference. *Q. Rev. Biol.* **66**: 411–453.

Hothorn, T., Bretz, F. & Westfall, P. 2008. *Simultaneous Inference in General Parametric Models*. Technical report number 019, Department of Statistics, University of Munich, München.

Howard, D.J. & Berlocher, S.H. (eds) 1998. *Endless Forms: Species and Speciation*. Oxford University Press, New York, NY.

Hoy, M.A. & Jeyaprakash, A. 2005. Microbial diversity in the predatory mite *Metaseiulus occidentalis* (Acari: Phytoseiidae) and its prey, *Tetranychus urticae* (Acari: Tetranychidae). *Biol. Control* **32**: 427–441.

Ito, K. & Fukuda, T. 2009. Molecular phylogeny of *Stigmaeopsis* spider mites (Acari: Tetranychidae) based on the cytochrome oxidase subunit I (COI) region of mitochondrial DNA. *Appl. Entomol. Zool.* **44**: 343–355.

Kimura, M. 1980. A simple method for estimating evolutionary rates of base substitutions through comparative studies of nucleotide sequences. *J. Mol. Evol.* **16**: 111–120.

Knegt, B., Potter, T., Pearson, N.A., Sato, Y., Staudacher, H., Schimmel, B.C.J. *et al.* 2017. Detection of genetic incompatibilities in non-model systems using simple genetic markers: hybrid breakdown in the haplodiploid spider mite *Tetranychus evansi*. *Heredity* **118**: 311–321.

Kosmidis, I. 2013. brglm: *Bias reduction in binomial-response Generalized Linear Models*. http://www.ucl.ac.uk/~ucakiko/software.html

Lukhtanov, V.A., Kandul, N.P., Plotkin, J.B., Dantchenko, A.V., Haig, D. & Pierce, N.E. 2005. Reinforcement of prezygotic isolation and karyotype evolution in *Agrodiaetus* butterflies. *Nature* **436**: 385–389.

Maheshwari, S. & Barbash, D.A. 2011. The genetics of hybrid incompatibilities. *Annu. Rev. Genet.* **45**: 331–355.

Malone, J.H. & Fontenot, B.E. 2008. Patterns of reproductive isolation in toads. *PLoS One* **3**: e3900.

Matsuda, T., Morishita, M., Hinomoto, N. & Gotoh, T. 2014. Phylogenetic analysis of the spider mite sub-family Tetranychinae (Acari: Tetranychidae) based on the mitochondrial COI gene and the 18S and the 5′end of the 28S rRNA genes indicates that several genera are polyphyletic. *PLoS One* **9**: e108672.

Matute, D.R. 2010. Reinforcement of gametic isolation in *Drosophila*. *PLoS Biol.* **8**: e1000341.

Moyle, L.C., Olson, M.S. & Tiffin, P. 2004. Patterns of reproductive isolation in three angiosperm genera. *Evolution* **58**: 1195–1208.

Navajas, M., Tsagkarakov, A., Lagnel, J. & Perrot-Minnot, M.-J. 2000. Genetic differentiation in *Tetranychus urticae* (Acari: Tetranychidae): polymorphism, host races or sibling species? *Exp. Appl. Acarol.* **24**: 365–376.

Nosil, P. & Crespi, B.J. 2006. Ecological divergence promotes the evolution of cryptic reproductive isolation. *Proc. R. Soc. Lond. B Biol. Sci.* **273**: 991–997.

Nosil, P. & Schluter, D. 2011. The genes underlying the process of speciation. *Trends Ecol. Evol.* **26**: 160–167.

Osakabe, M. & Komazaki, S. 1996. Host range segregation and reproductive incompatibility among *Panonychus citri* populations infesting osmanthus trees and other host plants. *Appl. Entomol. Zool.* **31**: 397–406.

Patten, M.M., Carioscia, S.A. & Linnen, C.R. 2015. Biased introgression of mitochondrial and nuclear genes: a comparison of diploid and haplodiploid systems. *Mol. Ecol.* **24**: 5200–5210.

Perrot-Minnot, M.-J., Migeon, A. & Navajas, M. 2004. Intergenomic interactions affect female reproduction: evidence from introgression and inbreeding depression in a haplodiploid mite. *Heredity* **93**: 551–558.

Pfennig, K.S. & Rice, A.M. 2014. Reinforcement generates reproductive isolation between neighbouring conspecific populations of spadefoot toads. *Proc. R. Soc. Lond. B Biol. Sci.* **281**: 20140949.

Presgraves, D.C. 2002. Patterns of postzygotic isolation in Lepidoptera. *Evolution* **56**: 1168–1183.

Price, T.D. & Bouvier, M.M. 2002. The evolution of F1 postzygotic incompatibilities in birds. *Evolution* **56**: 2083–2089.

Price, C.S.C., Kim, C.H., Gronlund, C.J. & Coyne, J.A. 2001. Cryptic reproductive isolation in the *Drosophila simulans* species complex. *Evolution* **55**: 81–92.

R Core Team. 2015. *R: A Language and Environment for Statistical Computing*. R Foundation for Statistical Computing, Vienna, Austria. http://www.R-project.org/.

Ros, V.I.D. & Breeuwer, J.A.J. 2009. The effects of, and interactions between, *Cardinium* and *Wolbachia* in the doubly infected spider mite *Bryobia sarothamni*. *Heredity* **102**: 413–422.

Rose, E.G., Brand, C.L. & Wilkinson, G.S. 2014. Rapid evolution of asymmetric reproductive incompatibilities in stalk-eyed flies. *Evolution* **68**: 384–396.

Saito, Y. 1995. Clinal variation in male-to-male antagonism and weaponry in a subsocial mite. *Evolution* **49**: 413–417.

Saitō, Y. 1990. 'Harem' and 'non-harem' type mating systems in two species of subsocial spider mites (Acari, Tetranychidae). *Res. Popul. Ecol.* **32**: 263–278.

Saito, Y. & Sahara, K. 1999. Two clinal trends in male-male aggressiveness in a subsocial spider mite (*Schizotetranychus miscanthi*). *Behav. Ecol. Sociobiol.* **46**: 25–29.

Saito, Y., Sato, Y., Chittenden, A.R., Lin, J.-Z. & Zhang, Y.-X. 2018. Description of two new species of *Stigmaeopsis*, Banks 1917 (Acari, Tetranychidae) inhabiting *Miscanthus* grasses (Poaceae). *Acarology*, **58**: 414–429, in press. https://doi.org/10.24349/acarologia/20184250.

Sakagami, T., Saito, Y., Kongchuensin, M. & Sahara, K. 2009. Molecular phylogeny of *Stigmaeopsis*, with special reference to speciation through host plant shift. *Ann. Entomol. Soc. Am.* **102**: 360–366.

Sakamoto, H., Matsuda, T., Suzuki, R., Saito, Y., Lin, J.-Z., Zhang, Y.-X. *et al.* 2017. Molecular identification of seven species of the genus *Stigmaeopsis* (Acari: Tetranychidae) and preliminary attempts to establish their phylogenetic relationship. *Syst. Appl. Acarol.* **22**: 91–101.

Sánchez-Guillén, R.A., Córdoba-Aguilar, A., Cordero-Rivera, A. & Wellenreuther, M. 2014. Genetic divergence predicts reproductive isolation in damselflies. *J. Evol. Biol.* **27**: 76–87.

Sasa, M.M., Chippindale, P.T. & Johnson, N.A. 1998. Patterns of postzygotic isolation in frogs. *Evolution* **52**: 1811–1820.

Sato, Y., Saito, Y. & Mori, K. 2000a. Patterns of reproductive isolation between two groups of *Schizotetranychus miscanthi* Saito (Acari: Tetranychidae) showing different male aggression traits. *Appl. Entomol. Zool.* **35**: 611–618.

Sato, Y., Saito, Y. & Mori, K. 2000b. Reproductive isolation between populations showing different aggression in a subsocial spider mite, *Schizotetranychus miscanthi* Saito (Acari: Tetranychidae). *Appl. Entomol. Zool.* **35**: 605–610.

Sato, Y., Saito, Y. & Chittenden, A.R. 2008. The parapatric distribution and contact zone of two forms showing different male-to-male aggressiveness in a social spider mite, *Stigmaeopsis miscanthi* (Acari: Tetranychidae). *Exp. Appl. Acarol.* **44**: 265–276.

Sato, Y., Egas, M., Sabelis, M.W. & Mochizuki, A. 2013a. Male–male aggression peaks at intermediate relatedness in a social spider mite. *Ecol. Evol.* **3**: 2661–2669.

Sato, Y., Sabelis, M.W. & Mochizuki, A. 2013b. Asymmetry in male lethal fight between parapatric forms of a social spider mite. *Exp. Appl. Acarol.* **60**: 451–461.

Sato, Y., Alba, J.M. & Sabelis, M.W. 2014. Testing for reproductive interference in the population dynamics of two congeneric species of herbivorous mites. *Heredity* **113**: 495–502.

Sato, Y., Breeuwer, J.A.J., Egas, M. & Sabelis, M.W. 2015. Incomplete premating and postmating reproductive barriers between two parapatric populations of a social spider mite. *Exp. Appl. Acarol.* **65**: 277–291.

Scopece, G., Musacchio, A., Widmer, A. & Cozzolino, S. 2007. Patterns of reproductive isolation in mediterranean deceptive orchids. *Evolution* **61**: 2623–2642.

Staudacher, H., Schimmel, B.C.J., Lamers, M.M., Wybouw, N., Groot, A.T. & Kant, M.R. 2017. Independent effects of a herbivore's bacterial symbionts on its performance and induced plant defences. *Int. J. Mol. Sci.* **18**: 182.

Takafuji, A. & Fujimoto, H. 1985. Reproductive compatibility between populations of the citrus red mite, *Panonychus citri* (McGregor) (Acarina: Tetranychidae). *Res. Popul. Ecol.* **27**: 361–372.

Tamura, K., Stecher, G., Peterson, D., Filipski, A. & Kumar, S. 2013. MEGA6: molecular evolutionary genetics analysis version 6.0. *Mol. Biol. Evol.* **30**: 2725–2729.

The Marie Curie Speciation Network 2012. What do we need to know about speciation? *Trends Ecol. Evol.* **27**: 27–39.

Thompson, J.D., Higgins, D.G. & Gibson, T.J. 1994. CLUSTAL W: improving the sensitivity of progressive multiple sequence alignment through sequence weighting, position-specific gap penalties and weight matrix choice. *Nucleic Acids Res.* **22**: 4673–4680.

Turelli, M., Lipkowitz, J.R. & Brandvain, Y. 2014. On the Coyne and Orr-igin of species: effects of intrinsic postzygotic isolation, ecological differentiation, X chromosome size, and sympatry on *Drosophila* speciation. *Evolution* **68**: 1176–1187.

Weeks, A.R., Velten, R. & Stouthamer, R. 2003. Incidence of a new sex-ratio-distorting endosymbiotic bacterium among arthropods. *Proc. R. Soc. Lond. B Biol. Sci.* **270**: 1857–1865.

Weisburg, W.G., Barns, S.M., Pelletier, D.A. & Lane, D.J. 1991. 16S ribosomal DNA amplification for phylogenetic study. *J. Bacteriol.* **173**: 697–703.

Werren, J.H., Baldo, L. & Clark, M.E. 2008. *Wolbachia*: master manipulators of invertebrate biology. *Nat. Rev. Microbiol.* **6**: 741–751.

Yano, J., Saito, Y., Chittenden, A.R. & Sato, Y. 2011. Variation in counterattack effect against a phytoseiid predator between two forms of the social spider mite, *Stigmaeopsis miscanthi*. *J. Ethol.* **29**: 337–342.

Yukilevich, R. 2012. Asymmetrical patterns of speciation uniquely support reinforcement in *Drosophila*. *Evolution* **66**: 1430–1446.

Zhang, Y.-K., Chen, Y.-T., Yang, K., Qiao, G.-X. & Hong, X.-Y. 2016. Screening of spider mites (Acari: Tetranychidae) for reproductive endosymbionts reveals links between co-infection and evolutionary history. *Sci. Rep.* **6**: 27900.

Zhou, W., Rousset, F. & O'Neill, S. 1998. Phylogeny and PCR-based classification of *Wolbachia* strains using *wsp* gene sequences. *Proc. R. Soc. Lond. B Biol. Sci.* **265**: 509–515.

Zhu, L.-Y., Zhang, K.-J., Zhang, Y.-K., Ge, C., Gotoh, T. & Hong, X.-Y. 2012. *Wolbachia* strengthens *Cardinium*-induced cytoplasmic incompatibility in the spider mite *Tetranychus piercei* McGregor. *Curr. Microbiol.* **65**: 516–523.

Supporting information

Additional Supporting Information may be found online in the supporting information tab for this article:

Table S1 Primers used in genetic analyses of *Stigmaeopsis micanthi* and in PCR assay for endosymbiont infection.

Table S2 Genetic distance in para-sodium channel gene of nDNA among populations calculated by the Kimura 2-parameter model.

Table S3 Genetic distance in COI gene of mtDNA among populations calculated by the Kimura 2-parameter model.

Table S4 Results of cross experiment and virgin oviposition.

Table S5 Quasibinomial generalized linear models in male offspring ratio to eggs as an index of postmating, prezygotic barrier, offspring mortality among diploid eggs as an index of postzygotic barrier, and values obtained by subtracting viable diploid offspring ratio from 1 as an index of total reproductive barrier with genetic distances

based on nDNA (para-sodium channel gene; A, B and C) and on mtDNA (COI; D, E and F).

Table S6 Analysis of deviance tables of quasibinomial generalized linear models (GLMs) for prezygotic barrier with geographic relationship, female form, genetic distance and the interactions, using dataset of HG and LW female populations from allopatric and parapatric areas (A). The genetic distance is based on nDNA (para-sodium channel gene) and mtDNA (COI). A saturated model based on mtDNA showed a marginally significant effect in the highest order interaction (A), therefore, the model was constructed in each HG and LW form females (B, C).

Figure S1 Maximum likelihood (ML) phylogenetic tree based on nDNA para-sodium channel gene (A) and mtDNA COI (B) of 12 *Stigmaeopsis miscanthi* populations and *S. longus* as the outgroup.

Figure S2 Results of PCR assay for *Wolbachia* infection in populations used in the cross experiments in which reproductive barriers were detected (LW2, LW4, HG2, HG4, ML3, and ML4).

Figure S3 Results of PCR assay for *Cardinium* infection in populations used in the cross experiments in which reproductive barriers were detected (LW2, LW4, HG2, HG4, ML3, and ML4).

Figure S4 Results of PCR assay for *Spiroplasma* infection in populations used in the cross experiments in which reproductive barriers were detected (LW2, LW4, HG2, HG4, ML3, and ML4).

Figure S5 Results of DNA extraction check using 28S rDNA in the females used in PCR assay for the endosymbiont infection.

Data deposited at Dryad: https://doi:10.5061/dryad.354f92m

Received 14 July 2017; revised 13 March 2018; accepted 15 March 2018